

of sodium ethoxide was added. Subsequently 12 mmol (2.02 g) of 1,3,5-benzenetri-methanol (synthesized as described previously¹⁸) were dissolved in 20 ml of dry THF. The reaction mixture was stirred at room temperature for approximately 2 hours. Subsequently 40 mmol (9.3 ml) of 3-aminopropyltriethoxysilane were added. The reaction mixture was allowed to stir at room temperature and was monitored by thin-layer chromatography. The crude product was redissolved in ether, and excess imidazole was removed via filtration. Purification by silica chromatography (Silica Gel 60 and 1.4/1.0 v/v hexane:ethyl acetate) resulted in a white wax-like solid (yield 55%).

Synthesis of silica

The amount of imprint used in the sol-gel synthesis corresponds to 2 mol% of imprint silicon relative to TEOS silicon. A typical procedure was to dissolve 0.7338 g of one-point imprint for one-point material synthesis (no imprint for control, 0.6532 g of two-point imprint and 0.6263 g of three-point imprint) into 193.5 ml of dry ethanol in a 16-ounce jar (Qorpak 7534). 23.0 ml of TEOS were added to this mixture. Finally 64.5 ml of pH 2.0 aqueous HCl were added to the gel mixture. The mixture was covered with a loose cap, stirred for 24 hours at 8 °C, stirred for 12 hours at 15 °C and for 8 days at room temperature. This mixture was transferred to a 40 °C oven. The mixture was aged in the oven for 10 days after which time gelation had occurred. The resulting glass monoliths were aged for 8 days at 40 °C. The final gels had an approximate imprint content of 0.283 mmol imprint nitrogen per gram of as-made material as determined from the mass balance. A thermogravimetric analysis (TGA) showed that the gels can be heated to over 200 °C in air without any detectable decomposition of imprint. The as-made imprinted silica monoliths were ground into a powder of particles less than 10 μm in diameter (verified by scanning electron microscopy). The powder was Soxhlet extracted with acetonitrile refluxing in calcium hydride. The silica was then separately washed with chloroform and pentane and allowed to dry. The silica was subsequently treated with an equimolar mixture of neat chlorotrimethylsilane and 1,1,1,3,3,3-hexamethyldisilazane at room temperature for 24 hours and finally was washed with dry THF, dry acetonitrile, chloroform, and pentane.

Procedures for imprint cleavage

15 ml per gram of silica of a 0.25 M trimethylsilyliodide in dry acetonitrile solution were added under argon to a batch of capped silica, and the resulting slurry was stirred in the dark for 12 hours under argon. Increasingly higher temperatures were used to effect deprotection in the multiple point materials; thus, 40 °C for the one-point material, 70 °C for the two-point material and 80 °C for the three-point material were used. The deprotected silica was collected by vacuum filtration and washed with dry acetonitrile, methanol, saturated aqueous sodium bicarbonate, methanol and acetonitrile. The deprotected silica was then Soxhlet extracted with acetonitrile refluxing in calcium hydride and chloroform and finally washed with pentane.

Catalytic reactions

1.5 mmol isophthalaldehyde and 3.0 mmol malononitrile were combined in 5ml acetonitrile containing 8 mg hexamethylbenzene as an internal standard and heated to 80 °C. Subsequently, 30 mg of imprinted silica (0.2 mmol amine per gram) or 6 mg of a surface-functionalized, amorphous silica (1 mmol amine per gram) were added and the progress of the reaction was monitored by gas chromatographic analysis.

Received 22 June; accepted 1 December 1999.

- Whitcombe, M. J., Rodriguez, M. E., Villar, P. & Vulfson, E. A new method for the introduction of recognition site functionality into polymers prepared by molecular imprinting - Synthesis and characterization of polymer receptors for cholesterol. *J. Am. Chem. Soc.* **117**, 7105-7111 (1995).
- Vlatakis, G., Anderson, L. I., Müller, R. & Mosbach, K. Drug assay using antibody mimics made by molecular imprinting. *Nature* **361**, 645-647 (1993).
- Wulff, G. Molecular imprinting in cross-linked materials with the aid of molecular templates - a way towards artificial antibodies. *Angew. Chem. Int. Edn Engl.* **34**, 1812-1832 (1995).
- Davis, M. E., Katz, A. & Ahmad, W. R. Rational catalyst design via imprinted nanostructured materials. *Chem. Mater.* **8**, 1820-1839 (1996).
- Shea, K. J. Molecular imprinting of synthetic network polymers: the de novo synthesis of macro-molecular binding and catalytic sites. *Trends Polym. Sci* **2**, 166-173 (1994).
- D'Souza, S. M. *et al.* Directed nucleation of calcite at a crystal-imprinted polymer surface. *Nature* **398**, 312-316 (1999).
- Shi, H., Tsai, W., Garrison, M. D., Ferrari, S. & Ratner, B. D. Template-imprinted nanostructured surfaces for protein recognition. *Nature* **398**, 593-597 (1999).
- Wulff, G., Heide, B. & Helfmeier, G. Molecular recognition through the exact placement of functional groups on rigid matrices via a template approach. *J. Am. Chem. Soc.* **108**, 1089-1091 (1986).
- Dai, S. *et al.* Imprint coating: A novel synthesis of selective functionalized ordered mesoporous sorbents. *Angew. Chem. Int. Edn Engl.* **38**, 1235-1239 (1999).
- Heilmann, J. & Maier, W. F. Selective catalysis on silicon dioxide with substrate-specific cavities. *Angew. Chem. Int. Edn Engl.* **33**, 471-473 (1994).
- Ahmad, W. R. & Davis, M. E. Transesterification on "imprinted" silica. *Catal. Lett.* **40**, 109-114 (1996).
- Maier, W. F. & Ben Mustapha, W. Transesterification on "imprinted" silica—Reply. *Catal. Lett.* **46**, 137-140 (1997).
- Katz, A. & Davis, M. E. Investigations into the mechanisms of molecular recognition with imprinted polymers. *Macromolecules* **32**, 4113-4121 (1999).
- Jones, C. W., Tsuji, K. & Davis, M. E. Organic-functionalized molecular sieves as shape-selective catalysts. *Nature* **393**, 52-54 (1998).
- Brinker, C. J., Keefer, K. D., Schaefer, D. W. & Ashley, C. S. Sol-gel transition in simple silicates. *J. Non-Cryst. Solids* **48**, 47-64 (1982).

- Fuji, K. *et al.* Visualization of molecular length of α,ω -diamines and temperature by a receptor based on phenolphthalein and crown ether. *J. Am. Chem. Soc.* **121**, 3807-3808 (1999).
- Dunn, D. & Zink, J. I. Probes of pore environment and molecule-matrix interaction in sol-gel materials. *Chem. Mater.* **4**, 2280-2291 (1997).
- Houk, J. & Whitesides, G. M. Structure reactivity relations for thiol disulfide interchange. *J. Am. Chem. Soc.* **109**, 6825-6836 (1987).

Acknowledgements

A Fannie and John Hertz Foundation Graduate Fellowship to A. K. and a NSF Waterman Award to M. E. D. are gratefully acknowledged. We thank L. W. Beck for assistance with the NMR experiments, and H. Gonzalez and A. G. Myers for discussions.

Correspondence and requests for materials should be addressed to M. E. D. (e-mail: mdavis@cheme.caltech.edu).

Biomimetic synthesis of ordered silica structures mediated by block copolypeptides

Jennifer N. Cha^{*}, Galen D. Stucky^{†*}, Daniel E. Morse[‡] & Timothy J. Deming^{†*}

Departments of ^{*}Chemistry, [†]Materials, and [‡]Molecular, Cellular and Developmental Biology, University of California, Santa Barbara, California 93106, USA

In biological systems such as diatoms and sponges, the formation of solid silica structures with precisely controlled morphologies is directed by proteins and polysaccharides and occurs in water at neutral pH and ambient temperature¹⁻⁴. Laboratory methods, in contrast, have to rely on extreme pH conditions and/or surfactants to induce the condensation of silica precursors into specific morphologies or patterned structures⁵⁻¹⁰. This contrast in processing conditions and the growing demand for benign synthesis methods that minimize adverse environmental effects have spurred much interest in biomimetic approaches in materials science^{4,5}. The recent demonstration that silicatein—a protein found in the silica spicules of the sponge *Tethya aurantia*¹¹—can hydrolyse and condense the precursor molecule tetraethoxysilane to form silica structures with controlled shapes at ambient conditions¹²⁻¹⁴ seems particularly promising in this context. Here we describe synthetic cysteine-lysine block copolypeptides that mimic the properties of silicatein: the copolypeptides self-assemble into structured aggregates that hydrolyse tetraethoxysilane while simultaneously directing the formation of ordered silica morphologies. We find that oxidation of the cysteine sulphhydryl groups, which is known to affect the assembly of the block copolypeptide¹⁵, allows us to produce different structures: hard silica spheres and well-defined columns of amorphous silica are produced using the fully reduced and the oxidized forms of the copolymer, respectively.

Because tetraethoxysilane (TEOS) is stable when mixed with water at neutral pH, a successful biomimetic silica synthesis from this precursor requires an agent that displays hydrolytic activity simultaneously with structure-directing properties. Site-directed mutagenesis of the cloned DNA coding for silicatein- α revealed that interacting histidine and serine residues were required for the hydrolytic activity of this protein^{4,14}. Based on this precedent, we evaluated simple homopolypeptides of amino acids bearing polar functional groups for their ability to mimic the properties of silicatein in the polycondensation of silicon alkoxides. When the homopolymers of L-lysine, L-histidine, D/L-serine, L-threonine and L-glutamic acid were separately dissolved in aqueous pH 7 buffer

Table 1 Block copolypeptides screened for their ability to react with TEOS to form silica

Block copolymer	Composition	Synthesis yield (%)	SiO ₂ rate		Shape	
			N ₂	Air	N ₂	Air
1	poly(L-alanine ₃₀ -b-L-lysine ₂₀₀)	87	0.09(2)	NA	N	NA
2	poly(L-glutamine ₃₀ -b-L-lysine ₂₀₀)	88	0.22(7)	NA	N	NA
3	poly(L-serine ₃₀ -b-L-lysine ₂₀₀)	84	0.29(3)	NA	N	NA
4	poly(L-tyrosine ₃₀ -b-L-lysine ₂₀₀)	86	0.30(7)	NA	N	NA
5	poly(L-cysteine ₁₀ -b-L-lysine ₂₀₀)	76	0.60(2)	0.60(2)	S	S
6	poly(L-cysteine ₃₀ -b-L-lysine ₂₀₀)	77	0.43(2)	0.62(4)	S	C
7	poly(L-cysteine ₆₀ -b-L-lysine ₂₀₀)	87	0.37(4)	0.67(1)	E	C
8	poly(L-cysteine ₃₀ -b-L-lysine ₄₀₀)	88	0.62(1)	0.65(4)	S	S
9	poly(L-cysteine ₃₀ -b-L-glutamate ₂₀₀)	90	0.01(1)	0.01(1)	NA	NA
10	poly(L-cysteine ₃₀)	76	0.43(6)	0.08(1)	N	N
11	poly(L-lysine ₂₀₀)	96	0.01(1)	NA	NA	NA
12	none	NA	0.01(1)	NA	NA	NA

Synthesis yield, total isolated yield of deprotected copolymer; SiO₂ rate, initial rate of silica formation (in $\mu\text{mol h}^{-1}$) mediated by block copolypeptide at a concentration of 5 mg ml^{-1} in 50 mM Tris-HCl buffer, pH 6.8 and an initial TEOS concentration of 3.4 M . The silica precipitate was collected by centrifugation, washed with 95% ethanol and dissolved in 0.2 M NaOH at 37°C . The amount of silica was then determined using the spectrophotometric molybdate assay^{24,25}. N₂ indicates that silica preparation was carried out under an oxygen-free nitrogen atmosphere; Air indicates that silica preparation was carried out in air. In the absence of polymer, buffer alone was used as the control. Shape, morphology of silica particles: N, non-ordered; S, spheres; E, elongated globules; C, columns. NA, not applicable; b, block copolymer.

and mixed with TEOS, it was found that none of these polymers was able to produce silica at ambient temperature over a 24-hour period. Furthermore, mixtures of these homopolymers also failed to catalyse TEOS hydrolysis and condensation. In contrast, we found that oligomers of L-cysteine (of molecular mass 3000 Da, used because higher chain lengths were insoluble) efficiently produce silica from TEOS in pH 7 buffer (Table 1), when handled under an inert nitrogen atmosphere to prevent oxidation. This result was presumably due to the nucleophilic properties of the sulphhydryl group, which may enable it to initiate hydrolysis of the silicon alkoxide. When these oligomers were used under air, oxidation of the sulphhydryl groups to disulphides resulted in insoluble aggregates that were much less active in silica formation (Table 1)¹⁶. However, the silica formed by using oligo-L-cysteine was an amorphous powder with no defined macroscopic shape. From these results we concluded that simple homopolymers of amino acids, which lack the structural complexity and polyfunctionality found in proteins, are unable to reproduce the shape-controlling ability of silicatein^{4,11–14}.

In an effort to better mimic this protein, we synthesized diblock copolypeptides that contained covalently linked domains (blocks) of water-soluble and water-insoluble polypeptides. Dissimilarity in the block segments gave the chains an amphiphilic character, similar to that of surfactants, which resulted in self-assembly of the chains in aqueous solution¹⁷. The architecture and design of the block copolypeptides also provided a means to solubilize water-insoluble domains; for example, hydrolytically active poly-L-cysteine. For

these reasons, block copolypeptides were expected to allow the directed cooperative assembly, hydrolysis and condensation of TEOS to form specific silica structures. The solubilizing block copolypeptide components were either cationic or anionic polyelectrolytes, such as poly-L-lysine and poly-L-glutamate, which are known to be water soluble at pH 7 (ref. 18). As water-insoluble domains, poly-L-cysteine and poly-L-serine were chosen both for their potential silica-forming hydrolytic activity as well as their ability to aggregate in water (by either hydrogen or covalent bonding via β -sheet formation or disulphide linkages¹⁶). Other insoluble domains chosen included polar residues that were less nucleophilic than cysteine (poly-L-glutamine and poly-L-tyrosine) or slightly hydrophobic (poly-L-alanine). Poly-L-histidine was not used in these studies because of difficulty in protecting the side-chain to form a suitable amino acid N-carboxyanhydride (amino acid NCA) monomer.

The block copolypeptides that were synthesized and studied are given in Table 1. They were prepared from suitably protected amino acid NCA monomers by using the initiator 2,2'-bipyridylNi(1,5-cyclooctadiene). This synthetic protocol has been shown to give block copolypeptides of narrow molecular mass distributions and with controlled molecular masses¹⁹ (Fig. 1).

The cationic block copolymers showed more activity in silica formation than the corresponding anionic copolymer. In fact, poly-L-glutamate completely inhibited the ability of the poly-cysteine block to form silica, which supports the hypothesis that polycations are important for interacting with negatively charged silicate

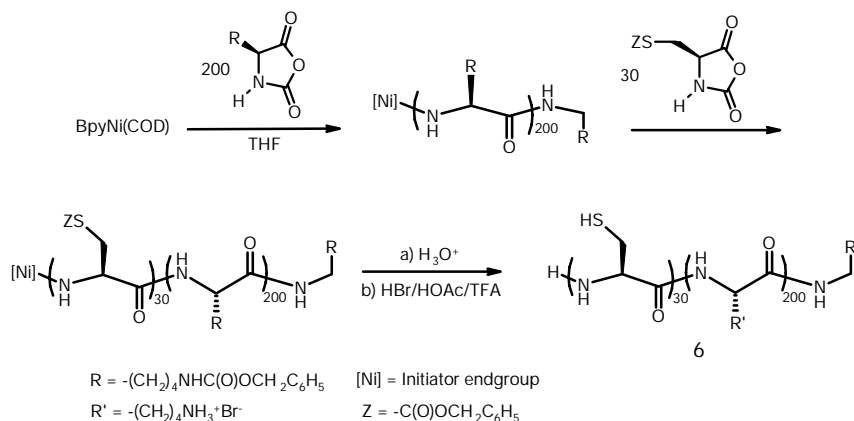


Figure 1 Synthesis strategy to produce block copolypeptides. Stepwise polymerization of the monomer, N ϵ -carboxybenzyl-L-lysine NCA, followed by S-carboxybenzyl-L-cysteine NCA gave the protected polymer that was then deprotected using equimolar amounts of trifluoroacetic acid and 33% HBr in acetic acid to give **6**. BpyNi(COD) indicates 2,2'-

bipyridylnickel(1,5-cyclooctadiene). The protected copolymer was analysed using size-exclusion chromatography in dimethylformamide (DMF) at 60°C to verify the molecular mass. Polymer composition was verified by $^1\text{H NMR}$ analysis of the deprotected copolymer in trifluoroacetic acid (TFA)-*d*

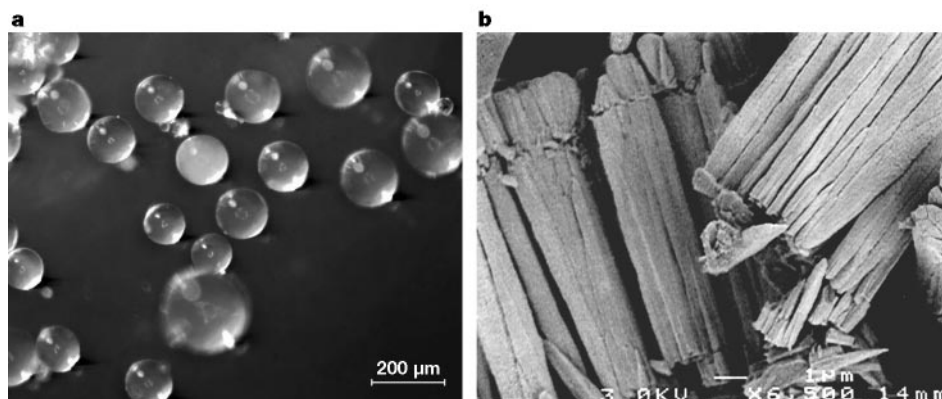


Figure 2 Different ordered silica shapes obtained using block copolypeptide **6**. In a typical procedure, TEOS (2.0 ml) was added to 500 μl of a solution of **6** (5 mg ml^{-1} in 50 mM Tris-HCl buffer, pH 6.8), and the resulting biphasic mixture was agitated vigorously and then allowed to stand for several hours with no stirring, whereupon some of the TEOS had emulsified into the aqueous phase. After 24 h, the resulting silica precipitate was collected from the aqueous phase, washed with 95% ethanol and air dried. **a**, Optical micrograph of

silica spheres obtained from synthesis under nitrogen; scale bar, 200 μm . **b**, Scanning electron micrograph of packed silica columns obtained from synthesis under air; scale bar, 1 μm . The sample was sputter coated with gold and examined with a JEOL JSM 6300F equipped with a cold cathode field-emission source operated at a beam energy of 3.0 kV.

precursors²⁰. All of the lysine-containing copolymers displayed some activity in silica formation, and the rate of silica production increased steadily as the domain bound to the poly-L-lysine block became more nucleophilic. As polymer **1** (see Table 1), which contains no nucleophilic component, was able to produce silica, it appeared that poly-L-lysine itself, when constrained in a self-assembling block copolymer, possessed a low activity toward the hydrolysis and condensation of TEOS. However, the cysteine- and serine-containing copolymers were the only ones that were able to control the shape of the silica during its formation, with the cysteine-containing polymers being most active. For these reasons, further studies were focused on the cysteine-lysine block copolymer combination.

In initial experiments, polymer **6** (polymers **1**–**12** are defined in Table 1) was deprotected and handled under a nitrogen atmosphere, and thus was used in its reduced form when reacted with TEOS. Dynamic light scattering measurements of **6** in aqueous solution (1.6 mg ml^{-1}) showed that this polymer self-assembled into large aggregates approximately 600 nm in diameter. This colloidal polymer solution, when mixed with TEOS, formed a two-phase system in which some TEOS was emulsified into the aqueous phase. After 24 hours, the formation of transparent, composite silica spheres (diameter, $\sim 100 \mu\text{m}$) was observed (Fig. 2). ²⁹Si magic-angle-spinning NMR measurements confirmed the existence of highly condensed silica (35% Q³ and 65% Q⁴ species). When calcined at 500 °C, the spheres remained both intact and transparent without a decrease in apparent size, although thermal gravimetric analysis revealed a 10% weight loss of organic material. Nitrogen sorption measurements using the BET (Brunauer–Emmett–Teller) showed that the spheres were mesoporous, with a broad distribution of pore sizes and a surface area of 436 m² g⁻¹ (ref. 21). Using the block copolypeptide **6** to prepare these hard, transparent, mesoporous silica spheres represents (to our knowledge) the first example in which hydrolysis and condensation of an inorganic phase as well as structural templating were all controlled by a single synthetic material at pH 7, thus mimicking biological silica synthesis. As far as we know, other surfactant or polymer based systems developed for shape-selective silica synthesis typically require use of a catalyst and extreme pH conditions^{10,22,23}.

Copolymers similar to **6**, but with different block lengths, were also synthesized to determine the role of copolymer composition on silica-forming ability. A polymer with a shorter cysteine domain, **7**, was similar to **6** in being able to produce silica spheres. However, when the length of the cysteine domain was increased (**8**), the

formation of more elongated silica particles was observed. Increasing the size of the lysine domain gave a polymer, **9**, which behaved in the same way as the smaller, but similar-composition, **7**. This indicates that the copolymer chain-length has little effect on resulting silica shape. It should be noted that mixtures of L-lysine and L-cysteine homopolymers, in proportions similar to those found in the block copolypeptides **6**–**9**, only gave completely disordered silica powders from TEOS.

An additional feature of the cysteine residues in **6** was their ability to form covalent disulphide bonds as inter- and intra-chain crosslinks upon oxidation of the sulphhydryl groups. After deprotection of the copolymer in air, the formation of such disulphide crosslinks in oxidized **6** was evident from the high viscosity exhibited by this sample upon exposure to water¹⁵. The gel dissolved readily upon addition of a reducing agent such as β -mercaptoethanol, indicating the presence of disulphide crosslinks¹⁵. Dynamic light scattering measurements of oxidized solutions of **6** showed that the block copolymer aggregates had increased in size (diameter $\sim 1,300 \text{ nm}$) relative to unoxidized samples ($\sim 600 \text{ nm}$). When oxidized **6** was mixed with TEOS, the rate of silica formation was found to increase, although 70% of the sulphhydryl groups had been converted to disulphide linkages (Table 1). In addition, ordered columns of silica were observed instead of spheres, showing that oxidation of the poly-L-cysteine domains was sufficient to completely modify the resulting topology of the silica (Fig. 2). With copolymers of different composition (Table 1), it could be shown that a minimum fraction of cysteine ($\sim 15 \text{ mol}\%$) was required to produce the columnar silica composites. These results illustrate the importance of the self-assembled block copolypeptide architecture in the formation of silica shapes. The synthetic capability to control directly silica shape, hydrolysis and condensation rate by adjustment of block copolypeptide composition that we report here offers a route to the environmentally benign, biomimetic synthesis of inorganic materials. □

Received 23 July; accepted 3 December 1999.

1. Simpson, T. L. & Volcani, B. E. *Silicon and Siliceous Structures in Biological Systems* (Springer, New York, 1981).
2. Kröger, N., Lehmann, G., Rachel, R. & Sumper, M. Characterization of a 200-kDa diatom protein that is specifically associated with a silica-based substructure of the cell wall. *Eur. J. Biochem.* **250**, 99–105 (1997).
3. Vrieling, E. G., Beelen, T. P. M., van Santen, R. A. & Gieskes, W. W. C. Diatom silicon mineralization as an inspirational source of new approaches to silica production. *J. Biotechnol.* **70**, 39–51 (1999).
4. Morse, D. E. Silicon biotechnology: harnessing biological silica production to make new materials. *Trends Biotechnol.* **17**, 230–232 (1999).

5. Mann, S. J. Biomimetic materials chemistry. *J. Mater. Chem.* **5**, 935–946 (1995).
6. Oliver, S., Kuperman, A., Coombs, N., Lough, A. & Ozin, G. Lamellar aluminophosphates with surface patterns that mimic diatom and radiolarian microskeletons. *Nature* **378**, 47–50 (1995).
7. Monnier, A. *et al.* Cooperative formation of inorganic-organic interfaces in the synthesis of silicate mesostructures. *Science* **261**, 1299–1303 (1993).
8. Zhao, D. Y. *et al.* Triblock copolymer syntheses of mesoporous silica with periodic 50 to 300 angstrom pores. *Science* **279**, 548–552 (1998).
9. Kresge, C. T., Leonowicz, M. E., Roth, W. J., Vartuli, J. C. & Beck, J. S. Ordered mesoporous molecular sieves synthesized by a liquid-crystal template mechanism. *Nature* **359**, 710–712 (1992).
10. Ying, J. Y., Mehnert, C. P. & Wong, M. S. Synthesis and applications of supramolecular-templated mesoporous materials. *Angew. Chem. Int. Edn Engl.* **38**, 56–77 (1999).
11. Shimizu, K., Cha, J., Stucky, G. D. & Morse, D. E. Silicatein alpha: cathepsin I-like protein in sponge biosilica. *Proc. Natl Acad. Sci. USA* **95**, 6234–6238 (1998).
12. Cha, J. N. *et al.* Silicatein filaments and subunits from a marine sponge direct the polymerization of silica and silicones in vitro. *Proc. Natl Acad. Sci. USA* **96**, 361–365 (1999).
13. Zhou, Y., Shimizu, K., Cha, J. N., Stucky, G. D. & Morse, D. E. Efficient catalysis of polysiloxane synthesis by silicatein alpha requires specific hydroxy and imidazole functionalities. *Angew. Chem. Int. Edn Engl.* **38**, 780–782 (1999).
14. Morse, D. E. Silicon biotechnology: proteins, genes and molecular mechanisms controlling biosilica nanofabrication offer new routes to polysiloxane synthesis. *Organosilicon Chemistry IV: from Molecules to Materials* (eds Auner, N. & Weis, J.) (Wiley-VCH, New York, in the press).
15. Liff, M. I. & Zimmerman, M. N. NMR Study of crosslinking by oxidation of four-cysteine polypeptide models of the elastic network phase of wool fibre. *Polym. Int.* **47**, 375–385 (1998).
16. Berger, A., Noguchi, J. & Katchalski, E. Poly-L-cysteine. *J. Am. Chem. Soc.* **78**, 4483–4488 (1956).
17. Zhang, L., Yu, K. & Eisenberg, A. Ion-induced morphological changes in crew-cut aggregates of amphiphilic block copolymers. *Science* **272**, 1777–1779 (1996).
18. Bamford, C. H., Elliot, A. & Hanby, W. E. *Synthetic Polypeptides* (Academic, New York, 1956).
19. Deming, T. J. Facile synthesis of block copolypeptides of defined architecture. *Nature* **390**, 386–389 (1997).
20. Mizutani, T., Nagase, H., Fujiwara, N. & Ogoshi, H. Silicic acid polymerization catalyzed by amines and polyamines. *Bull. Chem. Soc. Jpn* **71**, 2017–2022 (1998).
21. Lukens, W. W. Jr, Schmidt-Winkel, P., Zhao, D., Feng, J. & Stucky, G. D. Evaluating pore sizes in mesoporous materials: a simplified standard adsorption method and a simplified Broekhoff-de Boer method. *Langmuir* **15**, 5403–5409 (1999).
22. Huo, Q. S., Feng, J. L., Schuth, F. & Stucky, G. D. Preparation of hard mesoporous silica spheres. *Chem. Mater.* **9**, 14–15 (1997).
23. Zhao, D., Yang, P. D., Huo, Q. S., Chmelka, B. F. & Stucky, G. D. Topological construction of mesoporous materials. *Curr. Opin. Solid State Mater. Sci.* **3**, 111–121 (1998).
24. Strickland, J. D. H. & Parsons, T. R. *A Practical Handbook of Seawater Analysis* 2nd edn (Fisheries Research Board of Canada, Ottawa, 1972).
25. Brzezinski, M. A. & Nelson, D. M. A solvent-extraction method for the colorimetric determination of nanomolar concentrations of silicic-acid in seawater. *Mar. Chem.* **19**, 139–151 (1986).

Acknowledgements

We thank M. Brzezinski and B. Chmelka for suggestions, and E. Skogen for the light microscopy pictures. This work was supported by the US Army Research Office Multi-disciplinary University Research Initiative, the US Office of Naval Research, the NOAA National Sea Grant College Program, the US Department of Commerce, the California Sea Grant College System, the MRSEC Program of the NSF to the UCSB Materials Research Laboratory, and the Dow Corning Corporation.

Correspondence and requests for materials should be addressed to T. J. D. (e-mail: tdeming@mrl.ucsb.edu).

Natural methyl bromide and methyl chloride emissions from coastal salt marshes

Robert C. Rhew, Benjamin R. Miller & Ray F. Weiss

Scripps Institution of Oceanography, University of California at San Diego, La Jolla, California 92093-0244, USA

Atmospheric methyl bromide (CH₃Br) and methyl chloride (CH₃Cl), compounds that are involved in stratospheric ozone depletion, originate from both natural and anthropogenic sources. Current estimates of CH₃Br and CH₃Cl emissions from oceanic sources, terrestrial plants and fungi, biomass burning and anthropogenic inputs do not balance their losses owing to oxidation by hydroxyl radicals, oceanic degradation, and consumption in soils, suggesting that additional natural terrestrial sources may

be important¹. Here we show that CH₃Br and CH₃Cl are released to the atmosphere from all vegetation zones of two coastal salt marshes. We see very large fluxes of CH₃Br and CH₃Cl per unit area: up to 42 and 570 μmol m⁻² d⁻¹, respectively. The fluxes show large diurnal, seasonal and spatial variabilities, but there is a strong correlation between the fluxes of CH₃Br and those of CH₃Cl, with an average molar flux ratio of roughly 1:20. If our measurements are typical of salt marshes globally, they suggest that such ecosystems, even though they constitute less than 0.1% of the global surface area², may produce roughly 10% of the total fluxes of atmospheric CH₃Br and CH₃Cl.

Field studies were conducted between June 1998 and June 1999 in two southern California coastal salt marshes: the Mission Bay marsh (32° 47' N, 117° 13' W) and the San Dieguito lagoon (32° 58' N, 117° 15' W). The climate at these locations is Mediterranean, with wet winters and dry summers. During the March to September growing season, the soils are typically hypersaline; this is because tidal sea water provides most of the soil moisture and because evaporation usually exceeds precipitation³. Study plots (Table 1) were chosen within predominant vegetation communities along a vertical zonation typical of California salt marshes, from the upper marsh (which is inundated only at the highest tides) down to the tidal channels which are devoid of vascular plants. Gas fluxes were measured using a dark static flux chamber⁴ which covers a surface area of 1 m² and encloses a volume of 850 litres; the large chamber size reduces possible 'edge effects' and allows for whole plants to be enclosed. Samples of air were extracted from the chamber, and

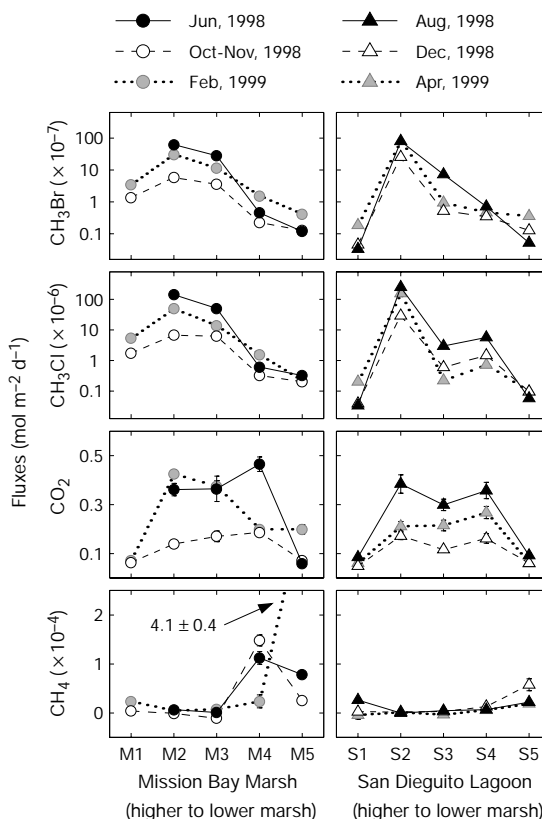


Figure 1 Daytime fluxes of CH₃Br, CH₃Cl, CO₂ and CH₄. Measurements were made between June 1998 and April 1999 at the Mission Bay marsh (circles, left panels) and the San Dieguito lagoon (triangles, right panels). Fluxes are highly variable, both seasonally and spatially, with the largest CH₃Br and CH₃Cl emissions from the upper-middle marsh during the growing season (March–September). The predominant types of vegetation and flux data for each site are listed in Table 1. Note the logarithmic scales for the CH₃Br and CH₃Cl fluxes. The error bars for CO₂ and CH₄ fluxes include analytical and curve-fitting errors.